A proposal for the generation of optical frequency comb in temperature insensitive microcavity*

Xun Lei(雷勋), Dandan Bian(边丹丹), and Shaowu Chen(陈少武)†

State Key Laboratory on Integrated Optoelectronics, Institute of Semiconductors, Chinese Academy of Sciences, Beijing 100083, *China*

(Received 6 May 2016; published online 30 September 2016)

We numerically simulate the generation of an optical frequency comb (OFC) in a microring based on the traditional Si_3N_4 strip waveguide and a temperature compensated slot waveguide. The results show that OFCs are susceptible to temperature with strip waveguide while they can keep stable when temperature changes 10 K in either low-Q (10^5) or high-Q (10^6) microcavity with the well-designed slot waveguide, which has great superiority in practical applications where the temperature drift of the cavity due to the intense pump or surrounding change is unavoidable.

Keywords: temperature insensitive, optical frequency comb, flattened dispersion, slot waveguide

PACS: 42.79.Nv, 42.79.Gn, 42.65.Yj **DOI:** 10.1088/1674-1056/25/11/114214

1. Introduction

Optical frequency combs (OFCs)[1,2] have become a powerful tool for high precision spectroscopy and are thereby used for various applications such as sensitive gas sensing,[3] molecular fingerprinting,[4] optical clocks,[5] and attosecond physics.[6] A monolithic frequency comb generator has been demonstrated for the first time in Ref. [7]. This approach is based on continuously pumped fused silica micro resonators on a chip, in which frequency combs are generated via parametric frequency conversion through four-wave mixing.[8] An important aspect of OFC in metrology is the stabilization of the comb repetition rate (f_r) and carrier envelope offset frequency (f_{CEO}).[8]

Due to the high pump power coupled into the resonator, the optical modes experience a significant thermal frequency shift as a result of the light absorption in the micro resonator. Usually the pump light is tuned into a resonance from high to low frequencies and the heating of the cavity is balanced by convective and conductive cooling, which allows for "thermal locking" [9–15] of the micro resonator mode to the pump laser and has been successfully used for self-stability of microcavities. Self-stability can compensate for various types of noise, but it cannot compensate a continuous slow drift, such as the case that the room temperature changes a few degrees.[10] What is more, it will be an unstable thermal equilibrium when the pump wavelength locates at the long wavelength side of the resonance wavelength, which is necessary in the generation of OFC on certain conditions. So we need some new approaches to stabilize the OFC. By using electronic feedback on both laser frequency and laser power, a micro resonator Kerr comb has been fully frequency stabilized with a relative accuracy of 10^{-16}.[12] However, this frequency stabilizing method is very complicated and expensive, which hinders some applications of the on-chip OFC such as multi-wavelength WDM light sources where the frequency stabilization is necessary but not as severe as those needed for high precise spectrum metrology. Therefore, a passive temperature compensation method is of great practical importance and highly desirable. In this work we numerically simulate the stability of OFC generated in a microring resonator based on a temperature-compensated silicon nitride slot waveguide.

2. Simulation results and discussion

We have recently designed a polyurethane acrylate (PUA)-cladding silicon nitride slotted waveguide,[16] which is shown in Fig. 1(b). Figure 1(a) shows the schematic structure of the all-pass microring resonator constructed by the PUA-cladding slotted waveguide on SiO_2 substrate which will be used as the core component of the OFC generator. The device is upper-cladded with lower refractive index material PUA, which has the thermo–optic coefficient of the opposite sign compared to that of the silicon nitride. Figure 1(c) shows a flat second-order dispersion curve covering a broad frequency band obtained in this waveguide, which is favorable to support broadband combs.[17–19] Figure 1(d) shows the effective refractive index of different waveguides as a function of temperature. We can get an almost completely athermal design of a PUA-cladding slotted silicon nitride waveguide with proper slot width and silicon nitride width. The thermo–optic coefficient ($\partial n_{\text{eff}}/\partial T$) is 3.8×10^{-5} K^{-1} for silicon nitride strip waveguide and 1.3×10^{-8} K^{-1} for the temperature-compensated silicon nitride slotted waveguide, corresponding to a resonant wavelength thermo-shifting rate of 32 pm/K and 0.01 pm/K near 1550 nm respectively when the radius of the

*Project supported by the National Natural Science Foundation of China (Grant Nos. 61435002, 61527823, and 61321063).

†Corresponding author. E-mail: swchen@semi.ac.cn

© 2016 Chinese Physical Society and IOP Publishing Ltd

microring is 100 μm. By comparing the two coefficients, the temperature-compensated silicon nitride slotted waveguide is much more temperature insensitive than the strip waveguide. In the following, we will investigate the influence of temperature change on the generation of OFC by numerical simulation.

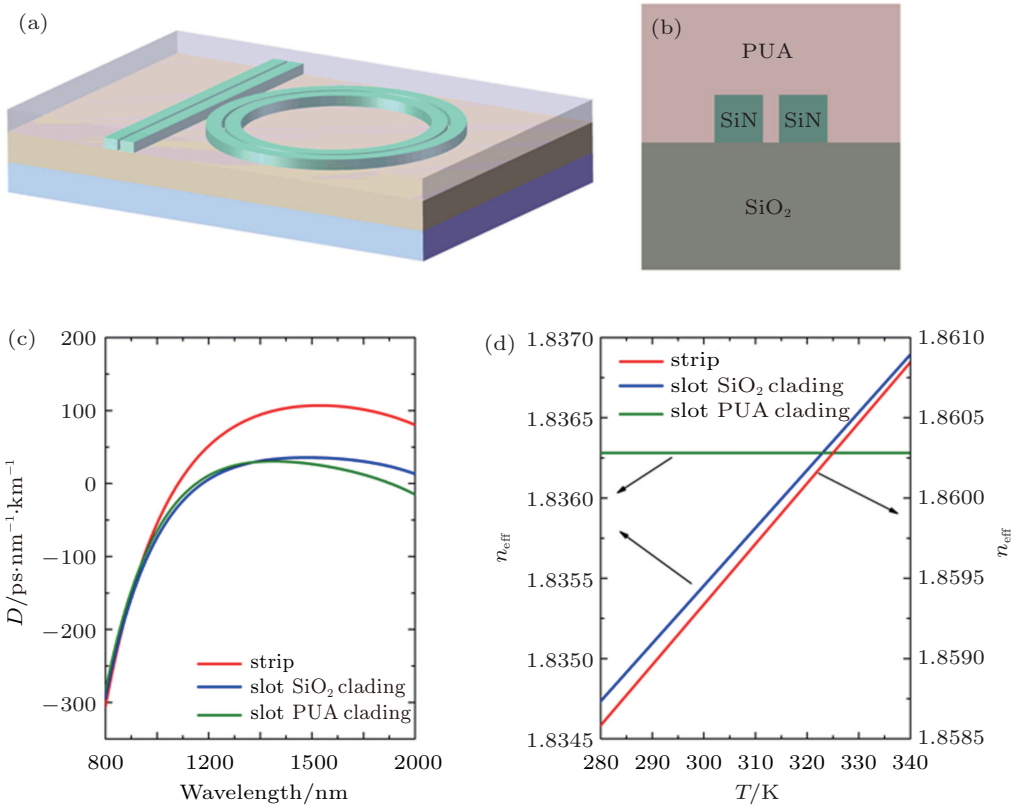


Fig. 1. (color online) (a) Schematic of an all-pass microring resonator constructed by PUA-cladding silicon nitride slotted waveguide. (b) The corresponding waveguide cross section. (c) Second-order dispersion versus wavelength for different waveguide. (d) Effective refractive index of the waveguide versus temperature. The red, blue, and green curves represent strip waveguide, slot waveguide with SiO_2 cladding, and slot waveguide with PUA cladding, respectively.

To numerically demonstrate the influence of the temperature change on OFC generation in different waveguides, we simulate the comb generation process using the Lugiato–Lefever equation[20,21]

$$\frac{\partial \psi}{\partial \tau} = -(1+\mathrm{i}\alpha)\,\psi + \mathrm{i}\,|\psi|^2\,\psi - \mathrm{i}\frac{\beta}{2}\frac{\partial^2 \psi}{\partial \theta^2} + F,$$

where the field envelope has been rescaled so that $\psi = (2g_0/\omega_0)^{1/2}A^*$ and the time has been rescaled so that $\tau = \omega_0 t/2$. The dimensionless parameters of this normalized equation are the frequency detuning $\alpha = -2\sigma/\omega_0$, the dispersion $\beta = -2\zeta_2/\omega_0$, and the external pump $F = (2g_0/\omega_0)^{1/2}f^*$.

Turing rolls and (bright) cavity solitons[21] are two important forms of OFC, which both are taken into account in our simulation. The initial cold cavity temperature is set to 300 K, and the dispersion of the strip waveguide and the slotted waveguide is 105.6 ps/(nm·km) and 28.7 ps/(nm·km), respectively. The quality factor is assumed to be 100000, which corresponds to a waveguide loss of ∼2 dB/cm.[22]

We set the initial detuning as −0.02 nm and OFC is stimulated from a cold cavity of 300 K. We then simulate the evolution of the OFC while the temperature changes slowly, as shown in Fig. 2(a). Figures 2(b) and 2(c) show the time domain and frequency domain status of the Turing rolls, and the spacing between the comb lines is 33 FSR (corresponding to the number of the "rolls" in time domain) at $3000\tau_{ph}$ and 34 FSR at $7000\tau_{ph}$. Even worse, when the temperature is further raised, such as at $11000\tau_{ph}$, the OFC will be substantially diminished, even to be vanished. Besides, the total intracavity energy[23] (denoted as U_{Intra}) at different time is also different. So we can conclude that the OFC is greatly influenced by the temperature change in traditional Si_3N_4 microcavity, even though the temperature shifting is merely a few tenths of one degree.

The fluctuation of temperature may cause the change of frequency detuning, and then results in the movement of OFC in the parameter space. The change of OFC mainly depends on its initial position in the parameter space and the variation of frequency detuning. So OFC is more susceptible to temperature in high Q microcavity due to its narrow mode bandwidth. To show the stability of OFC generated in the temperature compensated slot waveguide, we also simulate the evolution of OFC in high Q microcavity. Comparing to the simulation in Fig. 2, the initial normalized detuning and the cavity tem-

perature keep the same but the temperature raises 10 K in the simulation of Fig. 3. The dynamic evolution of OFC is shown in Fig. 3.

The blue dotted curve in Fig. 3 represents the intracavity energy of Turing rolls when $Q = 10^5$ and it is almost invariable when temperature changes a lot. The blue solid curve represents the case of $Q = 10^6$. Figures 3(b) and 3(c) represent the corresponding time domain and frequency domain status. The spacing between the comb lines keeps 19 FSR, but the power in time domain suffers a small decrease when temperature raises 10 K.

Comparing Figs. 2 and 3, we can make a conclusion that the microring based on temperature compensated slot waveguide is much more temperature insensitive in the dynamic evolution of Turing rolls. The Turing rolls is almost unchanged in the slot waveguide when the temperature rises for 10 K in the low-Q microcavity, while it varies obviously in the strip waveguide though the temperature raises only 0.25 K. What is more, Turing rolls in the slot waveguide still keep an acceptable stability in the high-Q cavity.

To show the influence of temperature on the evolution of soliton, we set the initial detuning as 0.03 nm and the process of simulation is similar to the above. First, we simulate the case for the traditional Si_3N_4 microcavity. The peak power of the soliton decreases while its duration increases as the temperature slowly drifts from 300 K to 300.25 K when the pump power is $F^2 = 4$. But the evolution of soliton is quite different when $F^2 = 4.5$. After a drastic oscillation, the single soliton splits into multi-solitons in time-domain and the envelope of the comb lines becomes irregular in the frequency domain when the temperature rises from 300.2 K to 300.25 K, as shown in Fig. 4(a).

Then, we deal with the case for the temperature compensated slot waveguide under the same initial detuning condition. The result of Fig. 5 indicates that the cavity soliton varies little in microring based on the temperature compensated slot waveguide when the temperature rises for 10 K. It shows that the microcavity based on the temperature compensated slot waveguide has a pretty good thermal stability compared with that based on the traditional Si_3N_4 microcavity.

The small dispersion of slot waveguide is not beneficial to getting natively mode-spaced (NMS) combs,[24] but its flattened anomalous dispersion profile allows for the generation of a broadband frequency comb. The most important is that OFC is nearly not influenced by the fluctuation of temperature in this waveguide. These characteristics may make the microcavity based on the slot waveguide an ideal device for the generation of OFC.

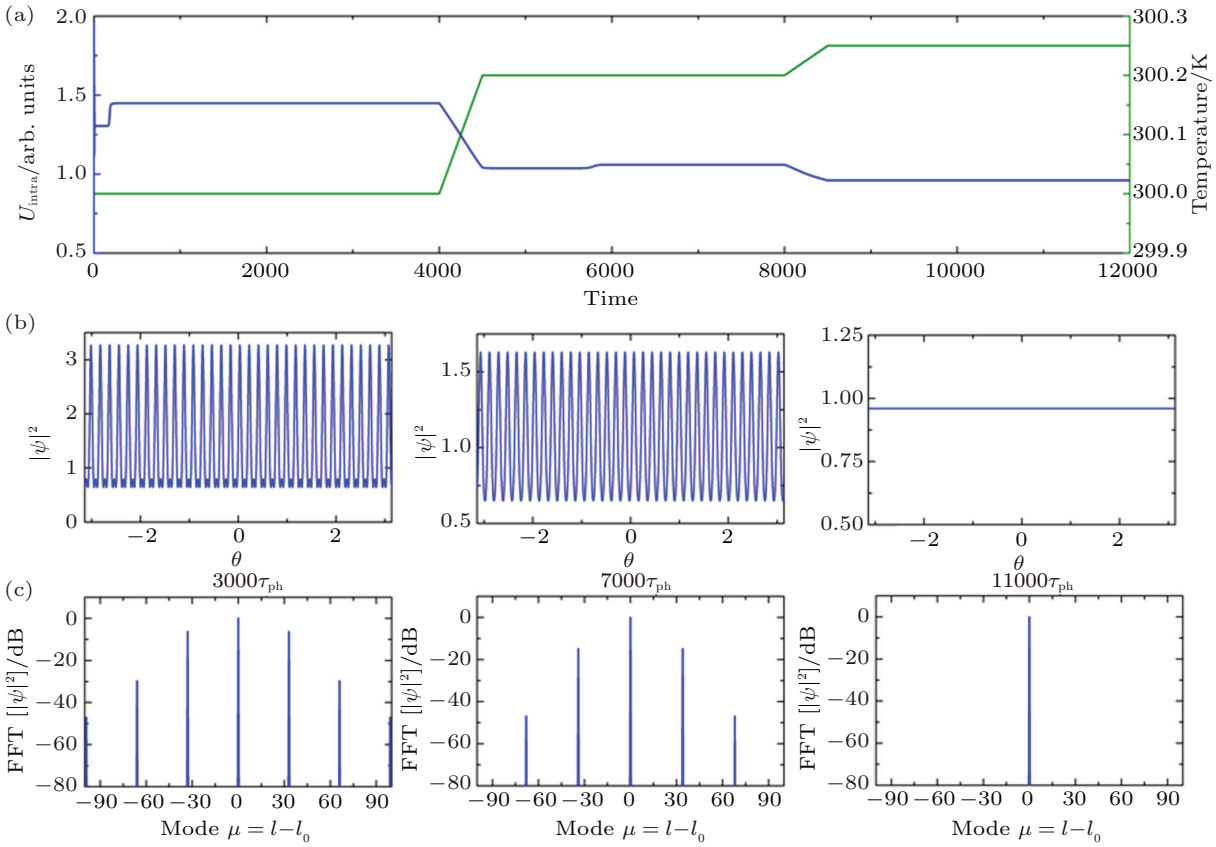


Fig. 2. (color online) (a) The temperature of the micro cavity (green curve) and the average round trip energy values of the cavity (blue). The horizontal axis is scaled in units of photon lifetime τ_{ph}. The time domain (b) and the corresponding frequency domain status (c) of the OFC at $3000\tau_{ph}$, $7000\tau_{ph}$, and $11000\tau_{ph}$, respectively. We denote the eigennumber of the pumped mode as l_0.

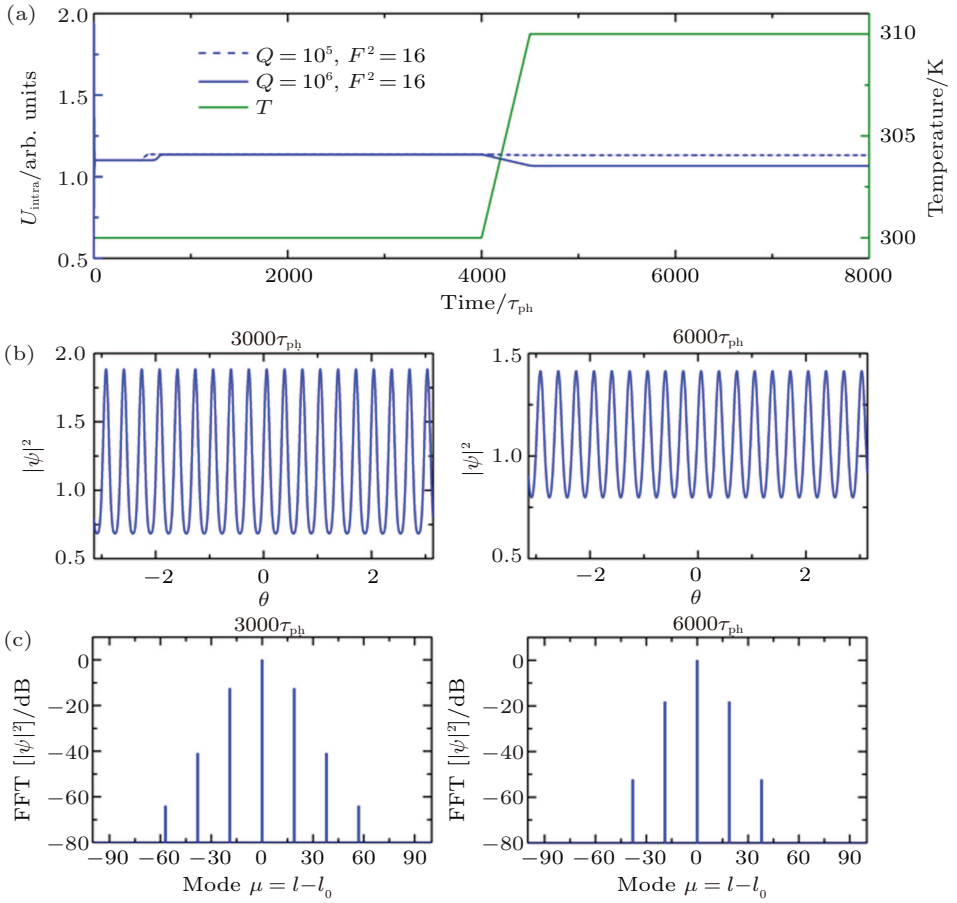


Fig. 3. (color online) (a) The temperature of the micro cavity (green curve) and the average round trip energy values of the cavity (blue). The time domain (b) and the corresponding frequency domain status (c) at $3000\tau_{\rm ph}$ and $6000\tau_{\rm ph}$ when $F^2=16$ in microcavities with $Q=10^6$.

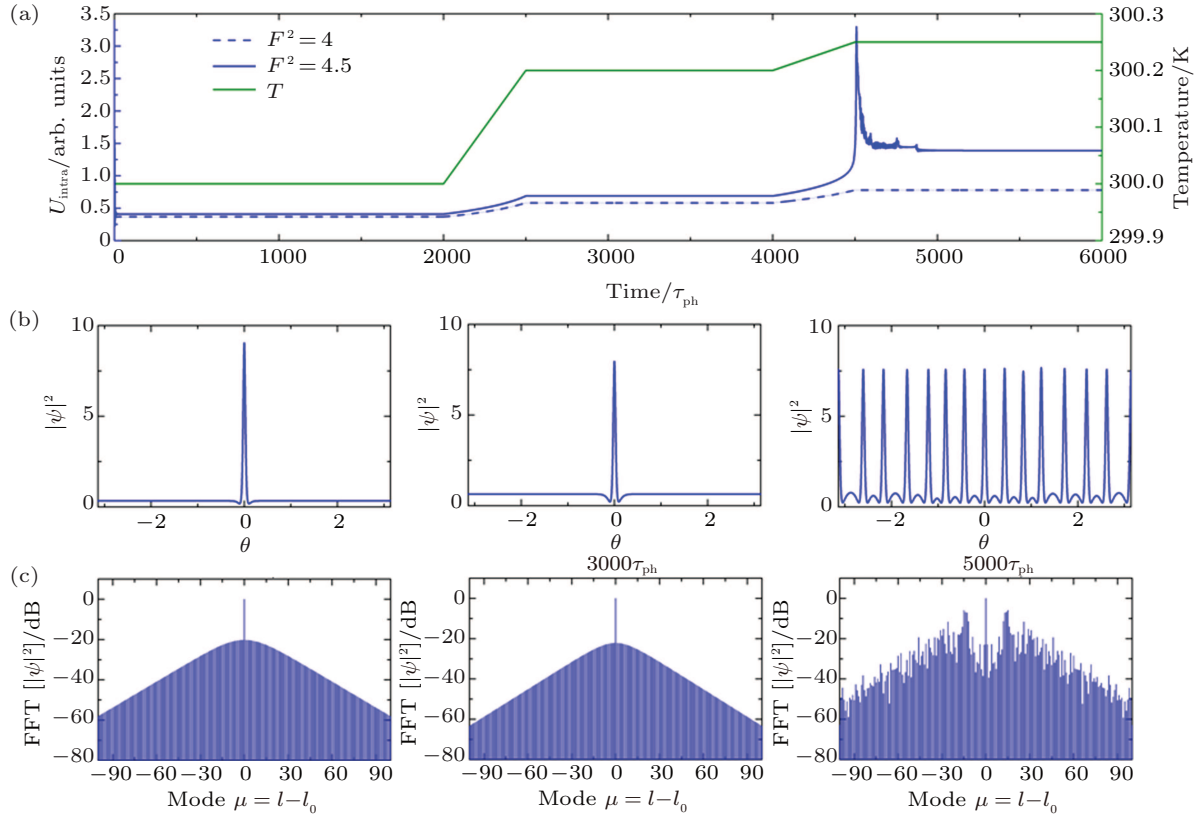


Fig. 4. (color online) (a) The temperature of the micro cavity (green curve) and the average round trip energy values of the cavity (blue). The blue solid line and the dotted line represent the different paths when the pump power is different. The time domain (b) and the corresponding frequency domain status (c) of the OFC at $1000\tau_{\rm ph}$, $3000\tau_{\rm ph}$, and $5000\tau_{\rm ph}$ when the pump power is $F^2=4.5$.

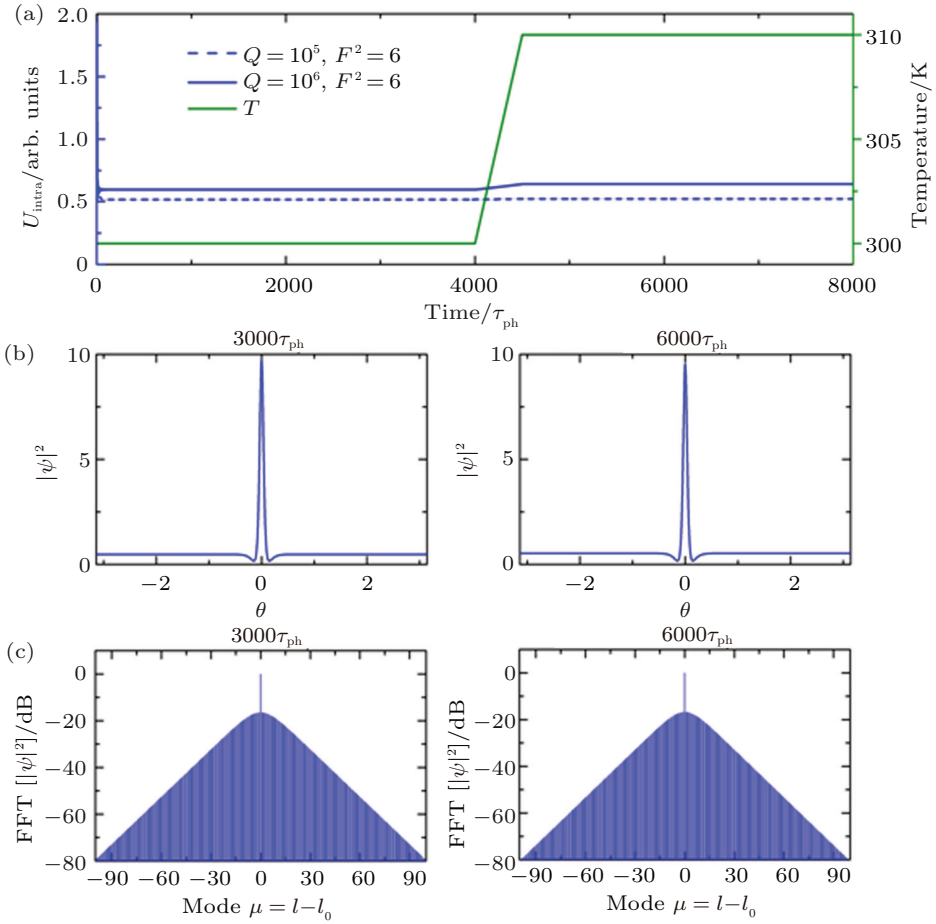


Fig. 5. (color online) (a) The temperature of the micro cavity (green curve) and the average round trip energy values of the cavity (blue). The time domain (b) and the corresponding frequency domain status (c) at $2000\tau_{\rm ph}$ and $6000\tau_{\rm ph}$ when $F^2=6$, $Q=10^6$.

3. Conclusion

We simulate the dynamic evolution of the Turing rolls and cavity soliton while the temperature changes slowly, which mimic the actual process. The results demonstrate that the microcavity based on the temperature compensated slot waveguide is much more temperature insensitive than the traditional strip waveguide. OFC stimulated from a microcavity based on the temperature compensated slot waveguide can keep stable when temperature raises 10 K. So the slot waveguide is of great practical importance in the application of OFC or other microcavity based optical devices.

References

[1] Holzwarth R, Udem T, Hänsch T W, Knight J C, Wadsworth W J and Russell P S J 2000 *Phys. Rev. Lett.* **85** 2264

[2] Diddams S A, Jones D J, Ye J, Cundiff S T, Hall J L, Ranka J K, Windeler R S, Holzwarth R, Udem T and Hänsch T W 2000 *Phys. Rev. Lett.* **84** 5102

[3] Thorpe M J, Moll K D, Jones R J, Safdi B and Ye J 2006 *Science* **311** 1595

[4] Diddams S A, Hollberg L and Mbele V 2007 *Nature* **445** 627

[5] Diddams S A, Udem T, Bergquist J C, Curtis E A, Drullinger R E, Hollberg L, Itano W M, Lee W D, Oates C W, Vogel K R and Wineland D J 2001 *Science* **293** 825

[6] Goulielmakis E, Yakovlev V S, Cavalieri A L, Uiberacker M, Pervak V, Apolonski A, Kienberger R, Kleineberg U and Krausz F 2007 *Science* **317** 769

[7] Del'Haye P, Schliesser A, Arcizet O, Wilken T, Holzwarth R and Kippenberg T J 2007 *Nature* **450** 1214

[8] Kippenberg T J, Holzwarth R and Diddams S A 2011 *Science* **332** 555

[9] Del'Haye P, Herr T, Gavartin E, Gorodetsky M L, Holzwarth R and Kippenberg T J 2011 *Phys. Rev. Lett.* **107** 063901

[10] Carmon T, Yang L and Vahala K J 2004 *Opt. Express* **12** 4742

[11] Grudinin I S, Yu N and Maleki L 2009 *Opt. Lett.* **34** 878

[12] Del'Haye P, Arcizet O, Schliesser A, Holzwarth R and Kippenberg T J 2008 *Phys. Rev. Lett.* **101** 053903

[13] Foster M A, Levy J S, Kuzucu O, Saha K, Lipson M and Gaeta A L 2011 *Opt. Express* **19** 14233

[14] Okawachi Y, Saha K, Levy J S, Wen Y H, Lipson M and Gaeta A L 2011 *Opt. Lett.* **36** 3398

[15] Levy J S, Gondarenko A, Foster M A, Turner-Foster A C, Gaeta A L and Lipson M 2010 *Nat. Photonics* **4** 37

[16] Bian D, Chen S, Lei X, Qin G and Chen Z 2016 *Appl. Opt.* **55** 4827

[17] Bao C, Zhang L, Matsko A, Yan Y, Zhao Z, Xie G, Agarwal A M, Kimerling L C, Michel J, Maleki L and Willner A E 2014 *Opt. Lett.* **39** 6126

[18] Zhang L, Bao C, Singh V, Mu J, Yang C, Agarwal A M, Kimerling L C and Michel J 2013 *Opt. Lett.* **38** 5122

[19] Bao C, Zhang L, Yan Y, Huang H, Xie G, Agarwal A, Kimerling L, Michel J and Willner A 2014 *CLEO: Scienceand Innovations,* June 8-13, 2014, San Jose, CA, p. SM1M. 5

[20] Coen S and Erkintalo M 2013 *Opt. Lett.* **38** 1790

[21] Chembo Y K and Menyuk C R 2013 *Phys. Rev. A* **87** 053852

[22] Zhang X, Liu T, Jiang J, Feng M and Liu K 2014 *Opt. Commun.* **332** 125

[23] Jaramillo-Villegas J A, Xue X, Wang P H, Leaird D E and Weiner A M 2015 *Opt. Express* **23** 9618

[24] Herr T, Hartinger K, Riemensberger J, Wang C Y, Gavartin E, Holzwarth R, Gorodetsky M L and Kippenberg T J 2012 *Nat. Photonics* **6** 480